

Kurt Stüwe

Effective bulk composition changes due to cooling: a model predicting complexities in retrograde reaction textures

Received: 12 March 1996 / Accepted: 7 April 1997

Abstract Diffusive processes are a strong function of temperature. Thus, during cooling of rocks, mineral grains may develop zoning profiles as successively larger parts of the grain “close” to the diffusive exchange with the rock. One of the consequences of this process is that, during cooling, successively larger parts of zoned minerals (depending on grain size) are effectively removed from the reacting part of the rock volume. Thus, the effective bulk composition of metamorphic rocks changes during cooling and the rate of its change will be a function of grain size. Because the sequence of metamorphic reactions seen by a given rock is a strong function of its bulk composition, this process may have the consequence that two rocks of *identical* overall bulk composition, but of different grain size, may experience a different sequence of reactions. Qualitatively *identical* peak paragenesis may therefore react to form qualitatively *different* retrograde reaction textures. The model is applied to examples in the pelitic system. There, garnet is usually the slowest diffusing phase developing zoning profiles during cooling and the effective removal of garnet from the reacting rock volume will cause changes of the effective bulk composition. It is shown that, during cooling of pelitic rocks from amphibolite facies conditions, typical aluminous peak parageneses of garnet-muscovite-kyanite \pm biotite may react to form either staurolite, chlorite or muscovite (or different combinations thereof), depending on grain size. During cooling from the granulite facies, aluminous peak parageneses of garnet-cordierite-sillimanite may form biotite, either on the expense of cordierite or garnet, also depending on grain size. The two examples are illustrated with a series of reaction textures reported for amphibolite and granulite terrains in the literature.

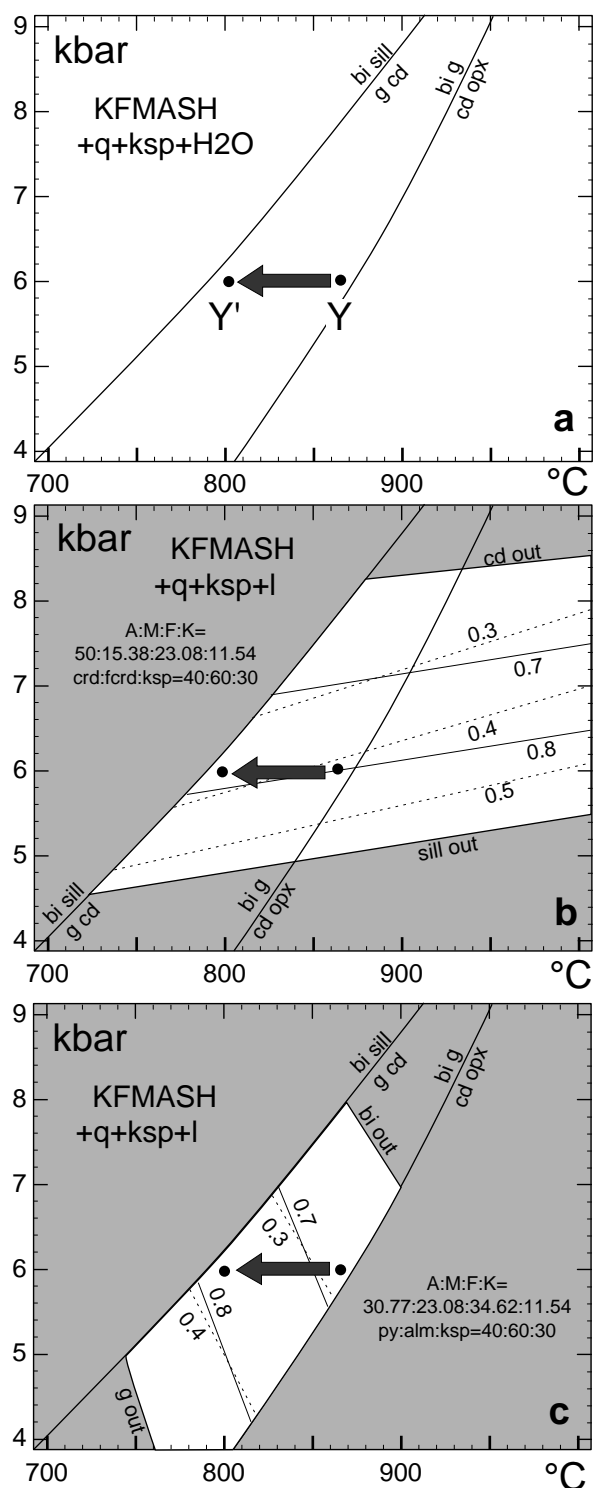
Introduction

Petrogenetic grids are one of the most important tools for the interpretation of pressure temperature (P, T) paths of metamorphic rocks. However, interpretation of these grids is often difficult, because they are projections of *all* phase equilibria information of a given model system onto the PT plane. Only a fraction of that information may be relevant for the interpretation of a given rock. For illustration, Fig. 1a shows part of a petrogenetic grid for high grade assemblages of the idealised pelitic system. This grid provides no information on the change of mineral equilibria for a rock that cooled along the hypothetical PT path $Y \rightarrow Y'$. In order to improve the interpretation, sections and pseudosections may be constructed (e.g. Hensen 1971). Petrogenetic PT pseudosections show only those equilibria that are relevant to a chosen bulk composition. The advantage of pseudosections over full petrogenetic grids is profound. In particular: (1) pseudosections only show system information pertaining to the interpretation of a given rock, thus, *all* information of the pseudosection may be used for interpretation; (2) details of continuous reaction of higher thermodynamic variance may be shown in pseudosections (Fig. 1b, c). The enormous advantage of pseudosections is only hampered by the need for knowledge of the relevant bulk composition. Discussion of this – and the size of the equilibration volume to derive it – is not a trivial task (see also Robinson 1991; Spear 1993) and it will be a major aim of this paper to draw the attention of the reader to the problems associated with its definition. Part of the problem is illustrated by a comparison of Fig. 1b and c. This shows two pseudosections of Fig. 1a, for two different bulk compositions of pelitic rocks. Figure 1b is for bulk compositions just *more* and Fig. 1c for bulk compositions just *less* aluminous than the garnet-cordierite tie line in AFM. Correspondingly, the two pseudosections show, respectively, a divariant field with the aluminous assemblage garnet-cordierite-sillimanite

K. Stüwe
Department of Earth Science, Monash University,
Clayton Vic. 3168, Australia

Editorial responsibility: V. Trommsdorff

(Fig. 1b) and garnet-cordierite-biotite (Fig. 1c). Contouring the divariant fields for isopleths in both pseudosections, shows an intriguing difference between the two equilibria. During cooling along the hypothetical path $Y \rightarrow Y'$ garnet and cordierite are predicted to become more Mg-rich in the bulk composition of Fig. 1b, but more Fe-rich in the bulk composition of Fig. 1c, assuming all phases are “communicating”.



This and similar examples in the literature (e.g. Robinson 1991), for example the observation of simultaneous consumption and precipitation of phases in different parts of a thin section (Foster 1991) highlight the importance of bulk composition to any consideration of PT paths. It is the focus of this paper to discuss aspects of its definition in a cooling rock.

The relevant bulk composition

The relevant bulk composition of a rock is that of the equilibration volume (e.g. Spear 1993). The equilibration volume is the volume of rock which, at a given P and T , reacts to be in chemical equilibrium. The bulk composition of this volume is the *effective bulk composition* (EBC) of the rock in this location. It need not be chemically isotropic – different minerals can be present – but each phase needs to be homogeneous. Zoned minerals represent, strictly, an infinity of EBC's and therefore equilibration volumes. If a pseudosection is to be constructed to interpret a rock, one of the hardest tasks is to identify this EBC. In the process of doing so, a series of untested assumptions about this process are (sadly) common practice. For example, on the scale of an outcrop it is common to consider rocks to be of different bulk composition. On the other hand, on the scale of a thin section, it is common to interpret all minerals to be in equilibrium i.e. of one bulk composition (given an “equilibrated” texture) and microprobe analyses from (often not even) adjacent grains are liberally used to identify the formation conditions. For “well-equilibrated” rocks both assumptions are probably useful, with the size of the equilibration volume being between thin section and outcrop scale. However, in rocks with reaction textures, i.e. rocks with *not* equilibrated textures, the definition of equilibrium volume becomes much harder and more crucial. There, textural contact is usually taken as an indicator for which minerals are in equilibrium and the problem of defining the EBC becomes apparent: the equilibration volume (and

Fig. 1 a Petrogenetic grid in system K₂O-FeO-MgO-Al₂O₃-SiO₂-H₂O (KFMASH) showing two reactions critical for high grade metamorphic assemblages. Mineral abbreviations are those of Holland and Powell (1990) and all diagrams are calculated with the software THERMOCALC (Powell and Holland 1988). **b**; **c** Show pseudosections of the grid in **a** for two different bulk compositions as given by A:F:M:K ratios and end member ratios. **b** is for bulk compositions just more aluminous than the garnet-cordierite tie line and shows, therefore, the divariant field $g-cd-sill$ ($+q+ksp+l$) (white field). **c** is for bulk compositions just less aluminous than the garnet-cordierite tie line and shows therefore the divariant field $g-cd-bi$ ($+q+ksp+l$). For simplicity the water activity in melt was assumed 1. The shaded regions depict trivariant fields and other divariant fields not shown here. X_{Fe} isopleths for garnet (solid thin lines) and for cordierite (dashed thin lines) are shown. Note that, for the same cooling path, ($Y - Y'$), garnet and cordierite will track towards more magnesium compositions in **b**, but towards more iron-rich compositions in **c**. (g garnet, cd cordierite, $sill$ sillimanite, q quartz, ksp k-feldspar, bi biotite)

therefore the EBC) lies somewhere between a single touching grain pair and the size of the thin section (see, Droop 1989). Unfortunately, it is only topologically possible to demonstrate contact equilibrium for at most four phases in a thin section (see discussion and references in Gardner 1980), while at least six phases are needed for a divariant equilibrium in a six component system (for example the idealised pelitic system). Reaction textures can therefore easily be misinterpreted in terms of an inappropriate bulk composition. This is particularly highlighted by detailed observations on mineral growth as a function of distance from some phases (e.g. Foster 1986; Yardley 1977). A discussion of the art of interpreting the equilibration volume from such observations lies well beyond the scope of this paper. However, a simple model will now be used to illustrate some of the effects that misjudgment of the equilibration volume may have.

Illustration with a model

Clearly, realistic equilibration volumes (and therefore EBC) are impossible to identify exactly. They will be of different size for different elements and they may exclude some slow diffusing phases near the texture of interest, but include rapidly diffusing phases far from it, for example because grain boundary diffusion is much more rapid than volume diffusion (Fig. 2). Moreover, catalysing processes may occur and fluids and deformation may play a role in determining the equilibration volume (Rubie 1986; Foster 1991). However, in order to illus-

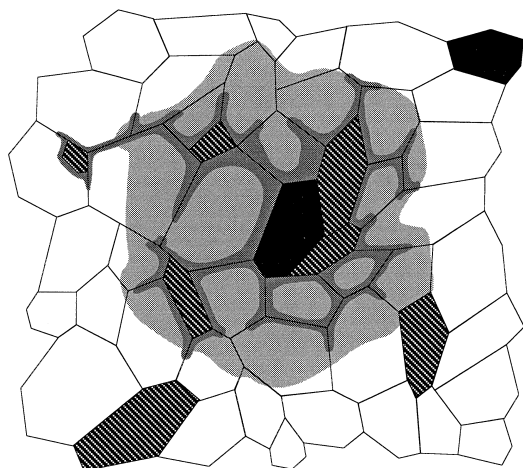


Fig. 2 A schematic thin section consisting of four different minerals, for example garnet (black), biotite (dashed) and a quartz-feldspar matrix (white). Superimposed is a “realistically” shaped equilibration volume for a given time at a given temperature (shaded lobate regions). Two different areas are shown to indicate, schematically, that the equilibration volume may be of different size for different elements. The smaller (darker shaded) region indicates the volume for an element in which the ratio of grain boundary diffusion to volume diffusion is larger than in the light-shaded equilibration volume. Thus, the dark-shaded volume extends along grain boundaries and includes only some “biotites” that can easily be reached along grain boundaries

trate how bulk compositions may differ for differently sized equilibration volumes, it suffices to use a simplistic model. It is assumed that the equilibration volume for a given time and at a given temperature, is a concentric sphere around the point of interest in a rock (Fig. 3). Using this model, the bulk compositional variation across a simple grain boundary can be investigated. Figure 3a shows a grain boundary superimposed by three different equilibration volumes. The parameter R is the radius of the equilibration volume and x is the distance of the point of interest from the grain boundary. It may be seen that, depending on R and x , the EBC changes between 100% phase A and 100% phase B . Figure 3b shows how this variation occurs for differently sized equilibration volume with radius R ; Fig. 3c shows how the bulk composition may change at one location in the thin section as a function of changing the size of the equilibration volume during temperature change (Appendix).

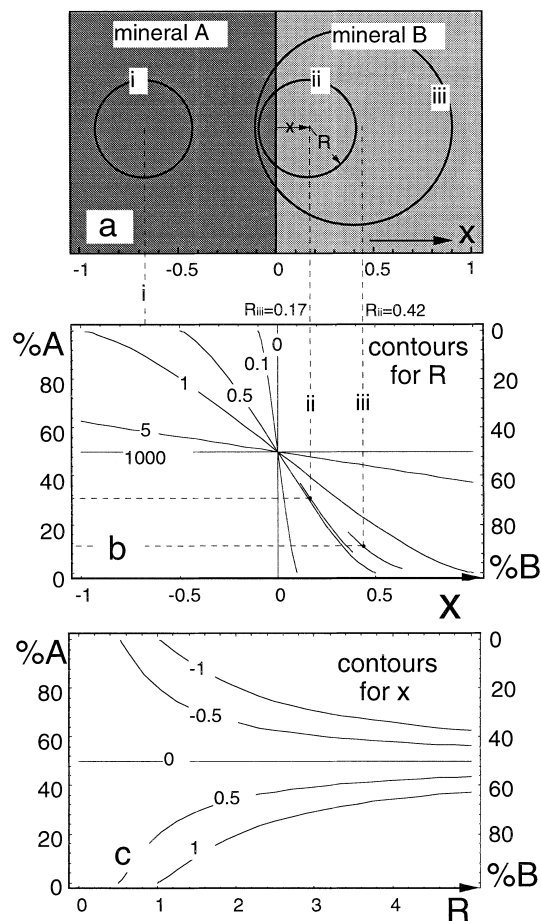


Fig. 3 a A schematic grain boundary between two minerals A and B . x is the distance of a point of interest from the grain boundary (measured positive towards grain B and negative towards grain A); R is the radius of the equilibration volume. b Shows the variation of bulk composition across the grain boundary for six differently sized equilibration volumes. c Shows the variation of bulk composition as a function of R (or temperature) for five different points of observation. The units for x are the same as those for R . Calculations are done with the relationship of the Appendix

Figure 4 illustrates the same two-phase model in two dimensions. The matrix phase *B* is kept white and a series of circular “porphyroblasts” of phase *A* are assumed to be embedded in it. Outside the shown area it is assumed that no further porphyroblasts occur. The contours show lines of constant bulk composition for a fixed *R*. Plots are shown for four different *R*. Clearly, for very small *R*, the bulk composition inside the porphyroblasts is near 100% *A* and in the matrix it is 100% *B*, except near the grain boundary. However, as the radius of the equilibration volume approaches the distance between two of the porphyroblasts, the amount of phase *A* in a given volume may come from more than one grain ($R = 2$). Therefore, the lines of constant bulk composition envelop more than one grain. For *R* much larger than the distance between porphyroblasts, the amount of *A* in the bulk composition approaches the average proportion of *A* in the rock. For example, on Fig. 4 for $R = 10$, the EBC is the same (6.8% of *A*) everywhere in the thin section. However, for intermediate *R*, lines of constant EBC show little apparent symmetry with the porphyroblast distribution ($R = 5$) and the EBC of the rock may be the same between grains and near grains. Interestingly, the direction of the composi-

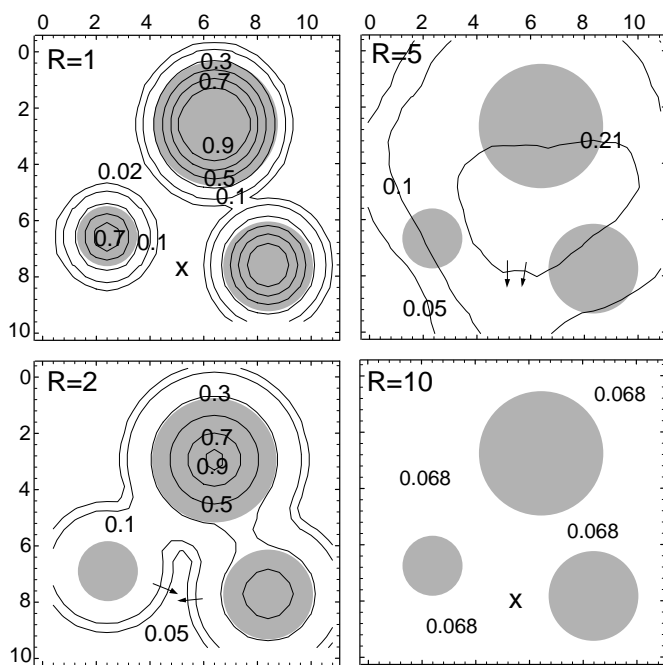


Fig. 4 A schematic thin section consisting of two minerals *A* (shaded circles) and *B* (white matrix) contoured for lines of constant bulk composition (contoured in proportion of *A*) for four different sizes of a circular model equilibration volume (characterised by *R* in length units). The radii of the “porphyroblasts” of phase *A* are 1; 1.5 and 2 units and the size of each plot is 10 length units. Note that the variation of bulk composition *and* the direction of the compositional gradient dramatically with *R*. For example, there is no compositional gradient at the marked location (cross) for very small ($R = 1$) or very large ($R = 10$) equilibration volumes; there is a steep horizontal gradient in opposing directions for $R = 2$ and there is a shallower but vertical gradient $R = 5$

tional gradient changes dramatically with changes in the size of the equilibration volume in parts of the plot (arrowed directions in Fig. 4 for $R = 2$ and $R = 5$). Considering that diffusion will, in general, occur at steep angles to isochemical surfaces, the rapid changes of isochemical contours on Fig. 4 predict complicated diffusion paths during temperature change.

Changes in bulk composition due to closing minerals

The discussion above has highlighted some of the problems associated with identifying the appropriate bulk composition of a reacting rock volume by taking an extremely simplistic view of the shape of the equilibration volume. In this section, this approach is refined by considering the effects of different diffusion rates in different phases to the equilibration volume.

Consider a pelitic rock containing garnet. Volume diffusion in garnet is likely to be the slowest diffusing process in such a rock and the diffusion properties of garnet will therefore limit the rate of equilibration of the rock. During cooling and “closure” of garnet (see, for example: Lasaga 1983; Spear 1993; Ehlers et al. 1994a), successively larger parts of garnet grains are effectively removed from the reacting rock volume composition and the EBC will change. An equivalent process may occur during the development of growth profiles on the heating path. This “prograde” process is known as Rayleigh fractionation and has been described in the literature for some time (e.g. Neumann et al. 1954; Hollister 1966, 1970; Loomis 1975; Robinson 1991). In the following, we concentrate on the effects of bulk composition changes during cooling.

For garnet-bearing rocks, the direction of EBC change during cooling must be on a line between the overall bulk composition and the equilibrium garnet, in direction away from the garnet. Details of the shape of the path of the changing EBC will depend on the reacting assemblage. As an example, consider the trivariant pelitic assemblage garnet-biotite (+ quartz + muscovite + H_2O) in the AFM (effectively mol $Al_2O_3:FeO:MgO$) projection (Fig. 5). During cooling from T_1 to T_2 , the garnet-biotite equilibrium will shift as indicated qualitatively by the tie lines (Fig. 5a). If this temperature change is associated with closure of part of the garnet, the EBC will shift towards biotite. During the same temperature change, the divariant equilibrium garnet-chlorite-biotite (+ quartz + muscovite + H_2O) will shift towards more Fe-rich compositions (e.g. Spear and Cheney 1989). Thus, it is possible that the divariant field will shift *over* the bulk composition of consideration (Fig. 5b). Chlorite will begin to grow. The compositional change of garnet in the divariant assemblage is qualitatively different from the trivariant assemblage and therefore the direction of compositional change of the EBC will change. Constructing this path of the EBC quantitatively would be extremely difficult (see discussion), but Fig. 5c shows one possible composite path

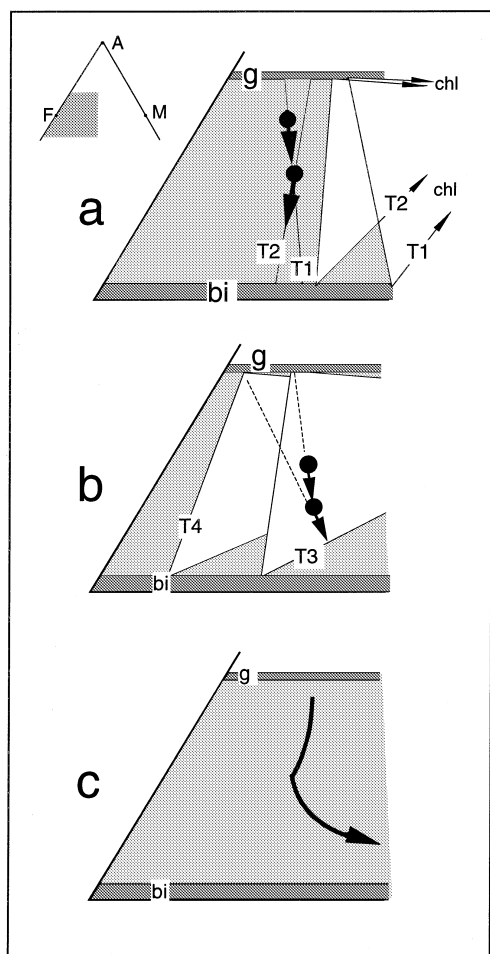


Fig. 5a-c Schematic AFM diagrams showing one possible change of EBC in pelitic rocks during cooling (trivariant fields shaded, divariant fields white). Only the section shaded in the inset is shown in a-c. **a** During cooling from T_1 to T_2 ($T_2 < T_1$) the equilibrium paragenesis is trivariant and – according to the shift of equilibrium tie lines – removal of garnet will result in a bulk composition vector away from garnet and with a clockwise rotational path. **b** During further cooling from T_3 to T_4 (with $T_4 < T_3 < T_2$), when the divariant tie triangle has shifted over the bulk composition, the changes of the EBC will be along an anticlockwise rotational vector. **c** Shows the composite path from **a** and **b**

(from Fig. 5a,b). Clearly, the shift of the EBC may result in other equilibria being intersected and it is, a priori, not clear what paragenetic effects this shift will cause in different parts of one thin section. It will be the subject of the remainder of this paper to consider the model discussed above with reference to a realistic example.

Application to an example in the pelitic system

As an example, consider amphibolite facies equilibria in the model system K_2O - FeO - MgO - Al_2O_3 - SiO_2 - H_2O (KFMASH). The phase diagram for this system is now well known (e.g. Spear and Cheney 1989; Xu et al. 1994) and forms therefore a good basis for application. Figure 6 shows a compatibility diagram for this system

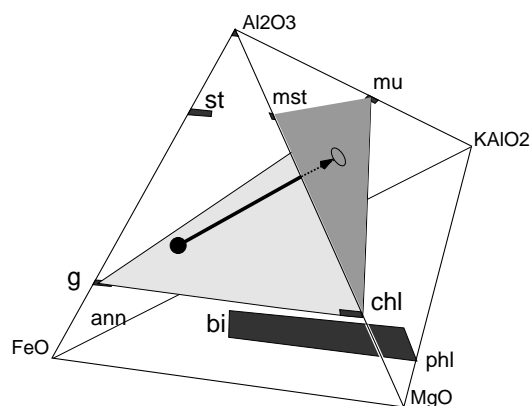
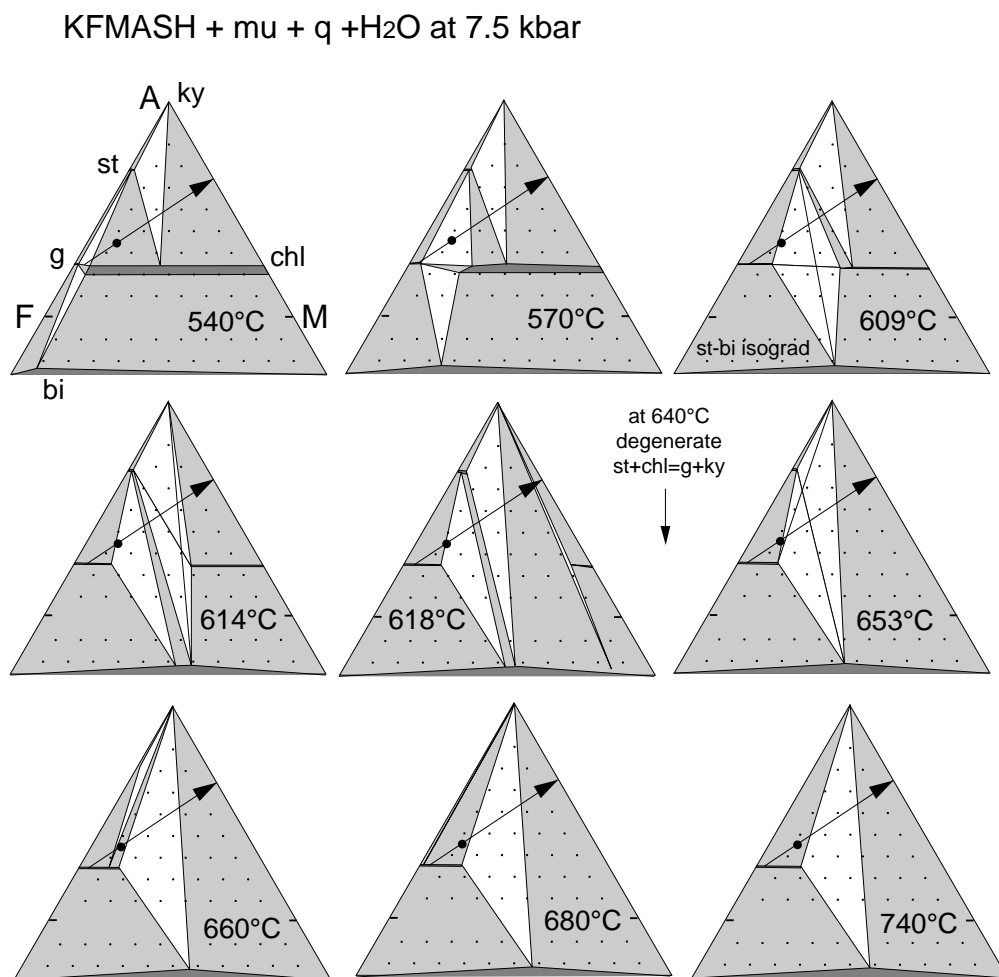


Fig. 6 Compatibility diagram for pelitic assemblages (+ q + H_2O) showing the compositional profile used in the $T - X_{EBC}$ section of Fig. 8 (arrows). The profile connects garnet (py:alm = 5:95) with a composition defined by the end members Mg-staurolite, amesite and muscovite (mst:ames:mu = 60:40:30) (dark shaded triangle) and is therefore appropriate to profiles with removal of garnet from a bulk composition at the black dot. The chosen bulk composition is just more aluminous than the garnet-chlorite-muscovite (g-chl-mu) tie plane (light shaded triangle)

illustrating an example of a *qualitatively* possible EBC path for a “normal” pelitic bulk composition (black dot) just *more* aluminous than the garnet-chlorite-muscovite tie plane. The path progresses in direction away from garnet, which is assumed to be the slowest diffusing phase in the assemblage. In order to perform calculations on the simplest level, details of the shape of the path of the EBC during cooling are neglected (for example due to compositional changes of garnet) and the path is assumed to be linear. This is justified, considering the small changes in equilibrium garnet composition in the T -range between 540 and 740 °C which will be our main focus below (e.g. Vance and Holland 1993). The far end of the path was chosen by an appropriate proportion of the end members mst (Mg-staurolite), ames (amesite) and mu (muscovite).

Figure 7 shows calculated mineral equilibria in KFMASH in AFM projections [projected from mu, q (quartz) and H_2O] at a series of different temperatures. Superimposed is the projected line of changing bulk composition (from Fig. 6). This vector connects a typical pelitic bulk composition of Al_2O_3 : MgO : FeO : K_2O = 32.77:10.72:55.22:1.3 with garnet. These ratios were chosen so that the bulk composition will feature roughly equal proportions of garnet, chlorite and staurolite in the divariant assemblage g-chl-st-mu-q- H_2O at intermediate PT around 570 °C and 7.5 kbar (see also: Figs. 7, 8). These component ratios lie on a direct line between garnet (py:alm = 5:95) and the end member combination mst:ames:mu = 60:40:30 and are representative of many amphibolite facies meta-pelitic schists. The calculations of Fig. 7 and all further calculations are performed with the software THERMOCALC (Powell and Holland 1988) using an updated version of the thermodynamic data set of Holland and Powell (1990; personal communication

Fig. 7 Calculated phase equilibria in the model system KFMASH at 7.5 kbar and 9 different temperatures shown in AFM compatibility diagrams projected from muscovite, quartz and H₂O. Quadrivariant assemblages are shaded dark, trivariant assemblages light and divariant assemblages are white. The degenerate reaction staurolite + chlorite → garnet + kyanite occurs at 640 °C but cannot be portrayed in a projection from muscovite and is therefore only schematically indicated. Phase equilibria were calculated with THERMOCALC (Powell and Holland 1988). The superimposed arrow is the EBC vector discussed in the text



1995). All assumptions about the formulation of end member activities, method of calculation and end member abbreviations are those of Stüwe and Powell (1995) and Xu et al. (1994). It may be seen that changes of the EBC in the shown temperature range interfere with changes of shifting equilibria. How these simultaneous changes may interfere is best shown on a $T - X_{\text{EBC}}$ section with the X_{EBC} -axis representing the changing EBC along the arrow in Fig. 7 due to removal of garnet. Interpretation of such a diagram will now be discussed.

Model predictions using $T - X_{\text{EBC}}$ sections

Figure 8 shows a $T - X_{\text{EBC}}$ section for amphibolite facies parageneses at 7.5 kbar in the idealised pelitic system. On this diagram, the X_{EBC} -axis corresponds to the bulk composition vector shown in Figs. 6 and 7. Assemblages become more garnet rich towards the left of the plot, terminating in the garnet-only quadrivariant one-phase field along the left margin. Towards the right, assemblages contain decreasing amounts of garnet and some assemblages are garnet free. Unlike Fig. 7, this diagram is not projected from muscovite and some

muscovite absent equilibria appear therefore which cannot be seen on Fig. 7. The bulk composition discussed above is indicated by the black triangle on the X_{EBC} -axis. Traditionally, any $T - X$ diagrams are interpreted along vertical paths (path (i), Figs. 8, 9), unless internal buffering mechanisms operate, as for example in $T - X_{\text{CO}_2}$ sections. Accordingly, meta-pelitic rocks of “normal” bulk composition that experienced metamorphism at 7.5 kbar and 700 °C and that contain the peak assemblage g-ky-mu, are predicted to form staurolite on the expense of kyanite, during initial cooling across the divariant field g-st-ky-mu. Further cooling across the g-st-chl-mu divariant field into the st-chl-mu trivariant field may result in chlorite growth on the expense of garnet.

However, if garnet is successively removed from the EBC due to the development of zoning profiles, then Fig. 8 has to be interpreted along paths that not only cool, but also change bulk composition, that is, from top left to bottom right (Figs. 8 and 9: path ii and iii). The steepness and curvature of the paths through this figure will depend on the degree of equilibration of garnets during cooling, and therefore on grain size, grain shape and cooling rate. In rocks with *small* grain size or *slow* cooling rate garnets may remain in equilibrium with the

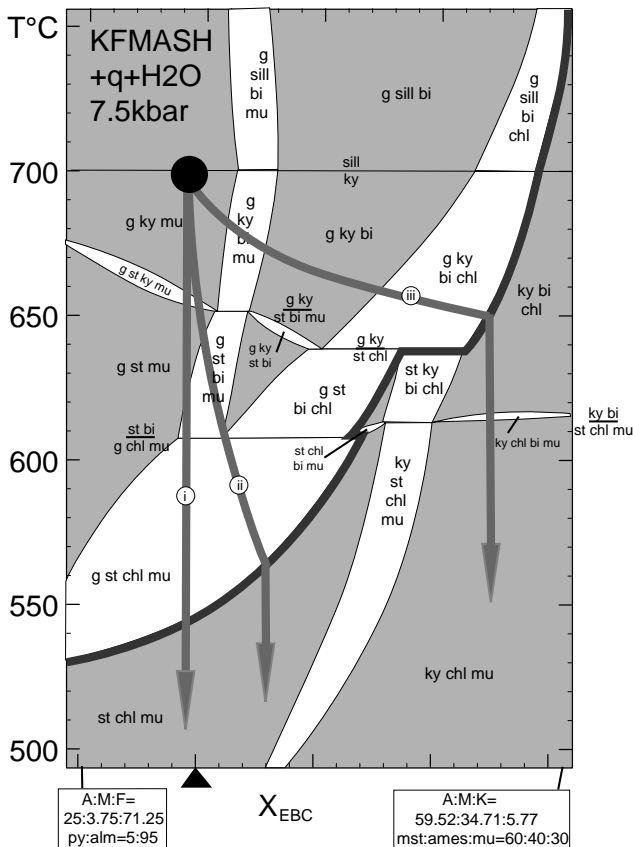


Fig. 8 $T - X_{\text{EBC}}$ section in KFMASH for amphibolite facies equilibria between g, ky, st, chl, bi, mu, q and H_2O at 7.5 kbar. The compositional (horizontal) axis was chosen on a line between “normal” pelitic bulk compositions just more aluminous than garnet-chlorite-muscovite and garnet. It corresponds to the vector in Fig. 7. The “normal” pelitic bulk composition chosen here is indicated by the black triangle. Divariant fields are white, trivariant fields are shaded. The thick black line is the stability limit of garnet. Paths (i), (ii) and (iii) refer to different rates of change of EBC during cooling. (ky kyanite, st staurolite, chl chlorite, mu muscovite)

whole rock to quite low temperatures (path ii). Then, the reaction sequence is largely similar to that of path (i). In rocks with large grain size or rapid cooling rate, on the other hand, garnets may close at significantly higher T and the changes of the EBC will occur at much higher T (path iii). Then, the peak assemblage g-ky-mu is predicted to first grow biotite on the expense of muscovite before growing chlorite on the expense of garnet. Once all garnet is removed from the EBC, cooling of all paths will continue along paths of constant EBC (Fig. 8) or depend on the diffusive properties of other minerals in the assemblage.

The model predicts therefore, that two rocks with the same overall bulk composition, but of different grain size, shape or cooling rate, may develop different retrograde assemblages. Different retrograde assemblages may therefore be expected between phases of apparently equivalent peak parageneses, if retrogradely zoned phases are present. The model appeals as it may, at least

in principle, explain some common observations in many rocks containing retrograde reaction textures.

Discussion, model problems and natural applications

In principle, it is possible to quantify EBC changes as a function of temperature and to calculate quantitative paths through $T - X_{\text{EBC}}$ diagrams. This would require implementation of diffusion processes under consideration of the appropriate boundary conditions, for example the description of finite grain sizes (e.g. Ehlers and Powell 1994) or mineral modes (Jenkin et al. 1995). However, it is believed that such calculations are unjustified in the light of other potentially important factors, for example the uncertainties associated with the knowledge of three dimensional grain size and shape in the analysis of thin sections (e.g. Ehlers et al. 1994a). In the following, some of the more fundamental model limitations are discussed, followed by qualitative model applications to natural examples from the literature.

Fluids, grain boundary diffusion or microcracking are likely to contribute to the transport of ionic species through a rock and therefore likely to contribute to the size of the equilibration volume. Indeed, fluids may enlarge the extent of the equilibration volume along grain boundaries to very large distances from the site of reaction. However, most of these processes are – like volume diffusion – also subject to a strong temperature dependence. Thus, they will also result in curved paths on $T - X$ sections and the main model conclusion remains valid. If, on the other hand, mass transfer is associated with fluid infiltration, metasomatic processes may occur and the system must be considered as an open system. Then, the EBC model cannot be applied.

The model is only valid for equilibration volumes that encompass a large number of grains. Then, removal of garnet will change the bulk composition significantly. The EBC would change much less if the equilibration volume is restricted to the grain boundaries of two co-existing minerals (Fig. 2). Thus, the model will only apply to reaction textures that involve participation of many mineral grains. Fortunately, the observation that di- and univariant reaction textures occur in metamorphic rocks (needing to involve at least six phases in the idealised system and more in realistic systems) indicates that this will, in general, be the case. Thus, realistic equilibration volumes do extend over a large number of grains, even if the mineral growth occurs only between two grains. Moreover, grain boundary diffusion is several orders of magnitude faster than volume diffusion. Therefore, surfaces of grains some distance away from a reaction site, but connected to it by grain boundaries, are likely to be part of the equilibration volume. Balancing reactions between products and reactants also shows, in general, that other phases further away from the site of mineral growth must have participated as reactants.

A drawback of interpreting the evolution of realistic PT paths on $T - X_{\text{EBC}}$ sections is that pressure changes, occurring simultaneously with EBC and T changes cannot be shown. For proper interpretation, a three dimensional diagram would be needed. However, if the PT path of a rock is known, then it is not difficult to calculate $(PT) - X$ diagrams, using a vertical axis which follows along the PT path.

Example from the amphibolite facies

Many examples from the literature show that amphibolite facies meta-pelitic rocks containing the peak metamorphic assemblage g-ky-mu \pm bi (+ q + H₂O) develop different combinations of staurolite, biotite and chlorite during cooling. It is also observed that the reaction textures ky \rightarrow st and mu \rightarrow bi often occur in the same thin section (e.g. Scottish Dalradian: Harte and Johnson 1969; Tauern window: Droop 1981, Figs. 3, 4; Koralm complex, eastern Alps: Stüwe and Powell 1995). In the following, we focus on a specific set of observations from the Koralm Complex in the Eastern Alps. There, amphibolite and eclogite facies metamorphic conditions around 700 °C and 14–17 kbar were reached in the Cretaceous (Frank et al. 1983) and garnet closure temperatures record the post peak cooling history from 700 to 400 °C, depending on grain size (Ehlers et al. 1994b). This large temperature interval during which closure of differently sized garnets occurred, indicates that EBC changes occurred during this whole T -interval. The retrograde PT path involved cooling and decompression (Thöni and Jagoutz 1992), probably preceded by an initial period of isobaric cooling (Stüwe and Powell 1995). Garnets in meta-pelitic rocks show complicated zoning patterns (e.g. Frank et al. 1983). Interpretation of the cooling history using Fig. 8 (being constructed for 7.5 kbar) is possible, because the qualitative sequence of the equilibria intersected by the PT path is largely independent of pressure (e.g. Stüwe 1994). Retrograde reaction textures in rocks containing the peak assemblage g-ky-mu include staurolite and biotite as reaction products from kyanite (and garnet), pervasive muscovite growth and minor chloritisation of garnet. Retrograde muscovite also grows as static porphyroblasts across the fabric and as reaction seams between kyanite and garnet. Muscovite is often mantled by late biotite with an $X_{\text{Fe}} = \text{Fe}/(\text{Fe} + \text{Mg}) = 0.4$. Biotite that grows after garnet is generally somewhat more Fe-rich with X_{Fe} around 0.5. These reaction textures have been widely described in the literature (e.g. Stüwe and Powell 1995, Fig. 2 and references therein) and are often observed within one thin section, but are incompatible with an interpretation along a single cooling path on Fig. 8. For example, the breakdown of kyanite and garnet to form staurolite and later chlorite predicts a vertical path (path i). On the other hand, growth of biotite near garnet and biotite on the expense of muscovite can only occur along a cooling path that is more

horizontal (path iii). It is suggested here that it is this type of observation that indicates that changes of the EBC occurred during cooling. This is supported by the composition of the late biotites around $X_{\text{Fe}} = 0.4$ which is incompatible with the equilibrium biotite composition in garnet-bearing equilibria (Fig. 7). Thus, both path (i) and path (iii) may both be appropriate to the cooling history of the g-ky-mu peak paragenesis, depending on the proximity to garnet crystals, garnet grain size and the degree of EBC changes during cooling.

Examples from the granulite facies

Pelitic rocks of many low pressure granulite facies terrains are characterised by the peak assemblage garnet-cordierite-sillimanite (+ q + ksp + l) (e.g. East Antarctica: Stüwe and Powell 1989; Broken Hill Block, Australia: Powell and Downes 1990; Central Australia: Dirks et al. 1991, Dronning Maud Land, Antarctica: Bucher-Nurminen and Ohta 1993; Jetty Peninsula, Antarctica: Hand et al. 1994). Because of the shallow level of metamorphism in these terrains, rapid cooling is probable and flat zoning profiles of garnets recording closure at high temperature is documented by most of these studies. This indicates that substantial changes of the EBC are likely, even at high temperatures. One common observation in retrograde reaction textures in these rocks is the occurrence of biotite that grew as a retrograde phase during cooling. This biotite growth occurs as reaction seams between garnet and cordierite, apparently on the expense of garnet, but often on the expense of cordierite, without apparent involvement of close-by garnet crystals. Thus, both stable coexistence of garnet-cordierite (with biotite growing within cordierite) and separation of the garnet-cordierite peak assemblage by biotite can be observed within the same thin section.

In order to investigate if this intriguing observation may be attributed to different EBCs in different parts of the same thin section, a $T - X_{\text{EBC}}$ section of granulite facies equilibria was constructed (Fig. 9). The EBC vector for this diagram was chosen to connect garnet and a bulk composition that contains the divariant assemblage g-cd-sill at 800 °C and 6 kbar. Figure 9 is therefore equivalent to Fig. 8 with EBCs involving decreasing amounts of garnet cooling along rightwards merging paths. In accordance with the peak conditions derived in most of the studies mentioned above, this figure shows that the peak assemblage g-cd-sill is stable above about 780 °C. The black dot was chosen to represent g-cd-sill as well as g-sill peak assemblages. Path (i) shows that, during cooling, rocks of constant EBC should develop biotite initially on expense of cordierite alone. Path (ii) shows that rocks with garnets closing at high temperature should develop biotite on expense of garnet. This is in perfect agreement with the observations recorded in many rocks that both the divariant fields g-bi-sill and cd-bi-sill may be crossed on the same cooling path by the same thin section.

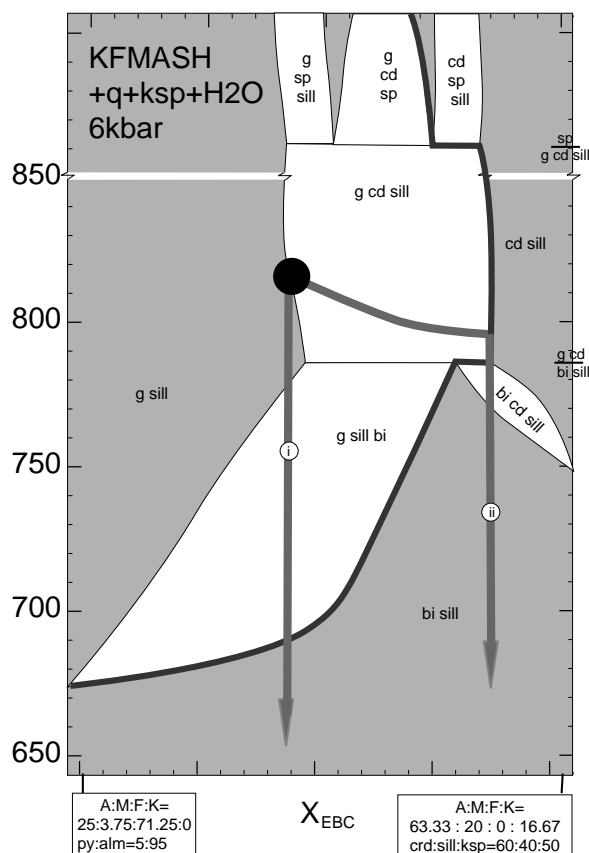


Fig. 9 $T - X_{EBC}$ section in KFMASH for granulite facies equilibria between g, cd, bi, sill, ksp, q and H_2O at 6 kbar. The compositional (horizontal) axis was chosen on a line between “normal” pelitic bulk compositions just more aluminous than garnet-cordierite and garnet. For field shading see Fig. 8. The thick black line denotes the stability limit of garnet

Concluding remarks

Development of zoning profiles in mineral grains during cooling implies that successively larger parts of these crystals are effectively removed from the reacting volume of the rock. Thus, the effective bulk composition of rocks may change during cooling. Because the sequence of metamorphic reactions during temperature change is a strong function of bulk composition, this process may control what retrograde reactions can occur. In the same way as diffusion processes control the “closure” of mineral grains, the rate of change of the bulk composition with cooling will depend: (1) on size and shape of mineral grains and grain boundary networks; (2) on cooling rate. As a consequence, two parts of a rock or thin section of identical whole rock composition, but of different grain size or shape, may record different retrograde mineralogies. This process may explain the common observations in metamorphic rocks that retrograde reaction textures *may* or *may not* be developed between the same peak paragenesis or that different retrograde parageneses occur between the same peak assemblage. In particular, the widely observed reaction

textures $ky \rightarrow st$ and $mu \rightarrow bi$ in g-ky-mu-q- H_2O peak assemblages of the amphibolite facies and $g \rightarrow bi$ or $cd \rightarrow bi$ in g-cd-sill-q-ksp-l peak assemblages of the granulite facies are incompatible with simple cooling paths on $T - X$ sections. It is this type of observation that indicates that partitioning and changing of the effective bulk composition occurs during cooling.

Appendix

The variation of bulk composition in the simple analytical model discussed on Figs. 3, 4 has been considered in two dimensions. That is, the equilibration “volume” has been considered as a circle. The parameter R is the radius of the equilibration volume, and x as the distance of the circle centre from a straight boundary between phases A and B , measured positive towards grain B . Then, the proportions of A in the bulk composition, X_A can be described by

$$X_A = \frac{A}{A+B} = \frac{1}{R^2\pi} \left(R^2 \text{ArcCos} \left(\frac{x}{R} \right) - x\sqrt{R^2 - x^2} \right)$$

as derived from simple geometrical consideration of Fig. 3a. An equivalent approach, summing the amounts of phase A from several porphyroblasts and taking account of the curved grain boundary, has been used to calculate Fig. 4.

Acknowledgements R. Powell is thanked for the many discussions on bulk compositions we have had over the years. T. Holland is thanked for the use of an unpublished update of the thermodynamic data set used by THERMOCALC. K. Ehlers is thanked for sharing with me many of her insights on the processes of diffusion and I. Buick and M. Hand are thanked for a series of discussions and a careful review of an early version of the manuscript. J. Ague, A. Feenstra and an anonymous reviewer are thanked for their very constructive criticisms during the review process.

References

- Bucher-Nurminen K, Ohta Y (1993) Granulites and garnet-cordierite gneisses from Dronning Maud Land, Antarctica. *J Metamorphic Geol* 5: 691–703
- Dirks PHGM, Hand M, Powell R (1991) The P - T -deformation path for a mid-Proterozoic, low-pressure terrane: the Tenolds Range, central Australia. *J Metamorphic Geol* 9: 641–661
- Droop GTR (1981) Alpine metamorphism of pelitic schists in the south-east Tauern window, Austria. *Schweiz Mineral Petrogr Mitt* 61: 237–273
- Droop GTR (1989) Reaction history of garnet-sapphirine granulites and conditions of Archaean high-pressure granulite facies metamorphism in the Central Limpopo Mobile Belt, Zimbabwe. *J Metamorphic Geol* 7: 383–405
- Ehlers K, Powell R (1994) An empirical modification of Dodson’s equation for closure temperature in binary systems. *Geochim Cosmochim Acta* 58: 241–248
- Ehlers K, Powell R, Stüwe K (1994a) Cooling rate histories from garnet + biotite equilibrium. *Am Mineral* 79: 737–744
- Ehlers K, Stüwe K, Powell R, Sandiford M, Frank W (1994b) Thermometrically inferred cooling rates from the Plattengneiss, Koralm region – Eastern Alps. *Earth Planet Sci Lett* 125: 307–321
- Foster CT (1986) Thermodynamic models of reactions involving garnet in sillimanite/staurolite schist. *Mineral Mag* 50: 427–439
- Foster CT (1991) The role of biotite as a catalyst in reaction mechanisms that form sillimanite. *Can Mineral* 29: 943–963

- Frank W, Esterlus M, Frey I, Jung G, Krohe A, Weber J (1983) Die Entwicklungsgeschichte von Stub- und Koralpenkristallin und die Beziehungen zum Grazer Palaeozoikum. In: Die früh-alpine Geschichte der Ostalpen. Jahresber Hochschulschwerpunkt, S15/4, pp 263–293
- Gardner M (1980) The coloring of unusual maps leads into uncharted territory. In: Mathematical games. *Sci Am* 242/2 pp 14–21
- Hand M, Scrimgeour I, Stüwe K, Powell R, Wilson CJL (1994) Metapelitic granulites from Jetty Peninsula, east Antarctica: formation during a single event or by polymetamorphism? *J Metamorphic Geol* 12: 557–573
- Harte B, Johnson MRW (1969) Metamorphic history of Dalradian rocks in Glens Clova, Esk and Lethnot, Angus, Scotland. *Scott J Geol* 5: 54–80
- Hensen BJ (1971) Theoretical phase relations involving cordierite and garnet in the system MgO-FeO-Al₂O₃-SiO₂. *Contrib Mineral Petrol* 92: 362–367
- Holland TJB, Powell R (1990) An enlarged and updated internally consistent thermodynamic dataset with uncertainties and correlations: the system K₂O-Na₂O-CaO-MgO-MnO-FeO-Fe₂O₃-Al₂O₃-TiO₂-SiO₂-C-H₂-O₂. *J Metamorphic Geol* 8: 89–124
- Hollister LS (1966) Garnet zoning: an interpretation based on the Rayleigh fractionation model. *Science* 154: 1647–1651
- Hollister LS (1970) Origin, mechanism and consequences of compositional sector zoning in staurolite. *Am Mineral* 55: 742–766
- Jenkin GRT, Rogers G, Fallick AE, Farrow CM (1995) Rb-Sr closure temperatures in bi-mineralic rocks: a mode effect and test for different diffusion models. *Chem Geol* 122: 227–240
- Lasaga AC (1983) Geospeedometry: an extension of geothermometry. In: Saxena SK (ed) Kinetics and equilibrium in mineral reactions. Springer Verlag, Berlin Heidelberg New York, pp 82–114
- Loomis TP (1975) Reaction zoning of garnet. *Contrib Mineral Petrol* 52: 285–308
- Neumann H, Mead J, Vitaliano CJ (1954) Trace element variation during fractional crystallization as calculated from the distribution law. *Geochim Cosmochim Acta* 6: 90–98
- Powell R, Downes J (1990) Garnet porphyroblasts-bearing leucosomes in meta-pelites: mechanisms, phase diagrams and an example from Broken Hill, Australia. In: Ashworth JR, Brown M (eds) High temperature metamorphism and crustal anatexis. The Mineralogical Society Series, no. 2, pp 105–123
- Powell R, Holland TJB (1988) An internally consistent thermodynamic dataset with uncertainties and correlations. 3. Application to geobarometry worked examples and a computer program. *J Metamorphic Geol* 6: 173–204
- Robinson P (1991) The eye of the petrographer, the mind of the petrologist. *Am Mineral* 76: 1781–1810
- Rubic DC (1986) The catalysis of mineral reactions by water and restrictions on the presence of aqueous fluid during metamorphism. *Mineral Mag* 50: 399–415
- Spear FS (1993) Metamorphic phase equilibria and pressure-temperature-time paths. Mineral Soc Am Monogr, Book Crafters, Chelsea, Michigan, USA
- Spear FS, Cheney JT (1989) A Petrogenetic grid for pelitic schists in the system SiO₂-Al₂O₃-FeO-MgO-K₂O-H₂O. *Contrib Mineral Petrol* 101: 149–164
- Stüwe K (1994) Some calculated thermodynamic pseudosections from the Plattengneiss and other rocks of the Koralm Complex, Eastern Alps. *Mitt naturwiss Ver Steiermark* 124: 29–39
- Stüwe K, Powell R (1989) Low pressure granulite facies metamorphism in the Larsemann Hills area, East Antarctica; petrology and tectonic implications for the evolution of the Prydz Bay area. *J Metamorphic Geol* 7: 465–483
- Stüwe K, Powell R (1995) *PT* paths from modal proportions: application to the Koralm Complex, Eastern Alps. *Contrib Mineral Petrol* 119: 83–93
- Thöni M, Jagoutz E (1992) Some new aspects of dating eclogites in orogenic belts: Sm-Nd, Rb-Sr, and Pb-Pb isotopic results from the Austroalpine Saualpe and Koralpe type locality (Carinthia/Styria, southeastern Austria). *Geochim Cosmochim Acta* 56: 347–368
- Vance D, Holland T (1993) A detailed isotopic and petrological study of a single garnet from the Gassetts Schist, Vermont. *Contrib Mineral Petrol* 114: 101–118
- Xu G, Will T, Powell R (1994) A calculated petrogenetic grid for the system KFMASH with particular reference to contact metamorphosed pelites. *J Metamorphic Geol* 12: 99–119
- Yardley BWD (1977) The nature and significance of the mechanism of sillimanite growth in the Connemara Schists, Ireland. *Contrib Mineral Petrol* 65: 53–58